

Supplementary information

Role of Er doping on isoamyl alcohol sensing performance of LaFeO₃ microspheres and its prospect in wheat mildew detection

Kaichun Xu^a, Mengjie Han^a, Zichen Zheng^a, Jinyong Xu^a, Marc Debliquy^b, Chao Zhang^a,

*

^a College of Mechanical Engineering, Yangzhou University, Yangzhou 225127, PR China

^bService de Science des Matériaux, Faculté Polytechnique, University of Mons, Mons 7000,
Belgium

* Corresponding author

Prof. Chao Zhang

College of Mechanical Engineering

Yangzhou University

Huayang West Road 196

Yangzhou 225127, Jiangsu Province

P.R. China

Tel/Fax: +86-514-87436008

Email: zhangc@yzu.edu.cn

Chemical Reagent

All the chemical reagents used in the preparation process of hydrothermal-synthesized LaFeO_3 powder were of analytical grade and used without further purification. Lanthanum nitrate hexahydrate ($\text{La}(\text{NO}_3)_3 \cdot 6\text{H}_2\text{O}$, 99%), Iron nitrate nonahydrate ($\text{Fe}(\text{NO}_3)_3 \cdot 9\text{H}_2\text{O}$, AR), Erbium nitrate hexahydrate ($\text{Er}(\text{NO}_3)_3 \cdot 6\text{H}_2\text{O}$, 99.99%), Citric acid ($\text{C}_6\text{H}_8\text{O}_7$, 99.5%) were all purchased from Shanghai Aladdin Biochemical Technology Co., Ltd.; Ethanol (99.7%) was supported by Chinasun Specialty Products Co., Ltd.

Synthesis of pure and Er-doped LaFeO_3

Firstly, x mmol $\text{Er}(\text{NO}_3)_3 \cdot 6\text{H}_2\text{O}$, $4-x$ mmol $\text{La}(\text{NO}_3)_3 \cdot 6\text{H}_2\text{O}$, and 4 mmol $\text{Fe}(\text{NO}_3)_3 \cdot 9\text{H}_2\text{O}$ ($x = 0, 0.04, 0.2, 0.4$) were dissolved successively in 40 mL of distilled water at room temperature. Then, 24 mmol citric acid was added to the above solution with stirring at 25°C for 10 min to obtain orange sol. Subsequently, the sol was transferred into a 100 mL Teflon-lined stainless autoclave and reacted at 180°C for 12 h. The precipitate was collected, washed three times with water and ethanol, dried at 70°C for 12 h, and then calcined at 700°C for 3 h. Finally, the brown pure and Er-doped LaFeO_3 powders were obtained. Interdigitated platinum electrodes used to fabricate gas sensors were fabricated by applying platinum paste to 6×30 mm alumina matrix through screen printing, and the spacing between the electrodes for gear shaping was 0.42 mm, as shown in Fig. S1.

Sample Characterization

Surface/cross-section morphologies, element content and distribution, and

lattice fringe gap were obtained by field emission scanning electron microscopy equipped with an energy dispersive spectrometer (FE-SEM, S4800II) and a high-resolution transmission electron microscope (HRTEM, Tecnai G2 F30). Phase and crystal structure parameters of gas sensing coatings and as-prepared powders were identified by X-ray diffraction analyzer (XRD, D8 Advance) with Cu-K α radiation. Element valence and oxygen vacancy content were acquired by X-ray photoelectron spectroscopy (XPS, ESCALAB 250Xi). The specific surface areas were calculated from nitrogen (N₂) adsorption/desorption isotherms (BET, Autosorb IQ3). The Er concentration of as-prepared samples were measured by inductively coupled plasma atomic emission (ICP-AES, Optima 7300 DV) to further verify whether the actual doping amount matches the preset value.

DFT simulations

The present first principle DFT calculations were performed by the Vienna Ab initio Simulation Package (VASP)¹ with the projector augmented wave (PAW) method.² The exchange-functional was treated using the generalized gradient approximation (GGA) of Perdew-Burke-Emzerhof (PBE) function.³ The energy cutoff for the plane wave basis expansion was set to 450 eV, and the force on each atom less than 0.05 eV/Å was set for the convergence criterion of geometry relaxation. Grimme's DFT-D3 methodology was used to describe the dispersion interactions.⁴ Partial occupancies of the Kohn-Sham orbitals were allowed using the Gaussian smearing method and a width of 0.05 eV. The Brillouin zone was sampled with Monkhorst mesh 2 \times 2 \times 1 through all the computational processes. The self-consistent

calculations applied a convergence energy threshold of 10^{-5} eV. A 15 Å vacuum space along the z direction was added to avoid the interaction between the two neighboring images.

The adsorption energy (E_{ads}) of isoamyl alcohol was defined as

$$E_{\text{ads}} = E_{\text{isoamyl alcohol/surf}} - E_{\text{surf}} - E_{\text{isoamyl alcohol(g)}}$$

where $E_{\text{isoamyl alcohol/surf}}$, E_{surf} , and $E_{\text{isoamyl alcohol(g)}}$ represented the energy of isoamyl alcohol adsorbed on the surface, the energy of clean surface, and the energy of isolated isoamyl alcohol molecule in a cubic periodic box, respectively.

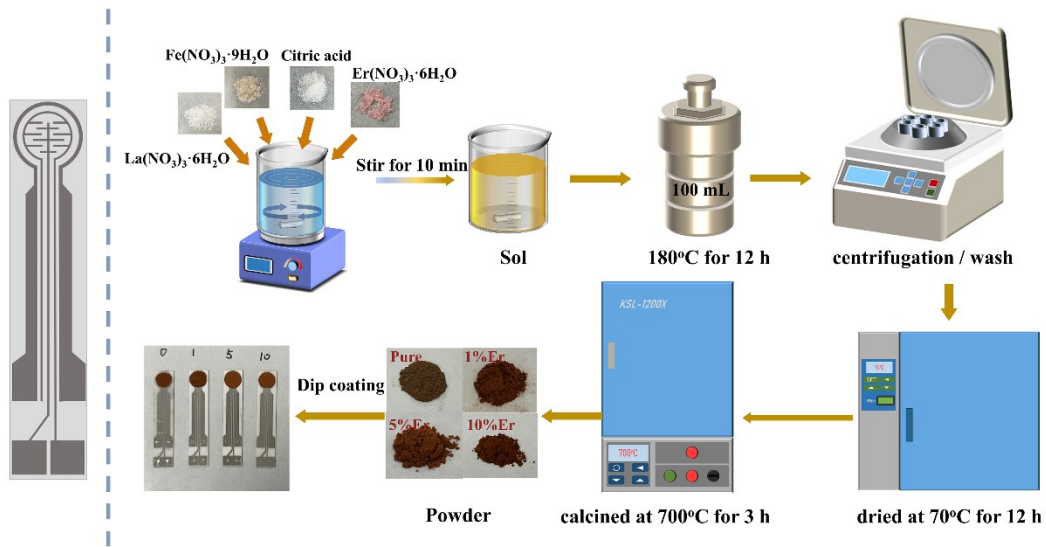


Figure S1. The interdigitated platinum electrode used in sensing measure (left), and schematic diagram of the hydrothermal synthesis procedure of the pure and Er-doped LaFeO₃ powders (right).

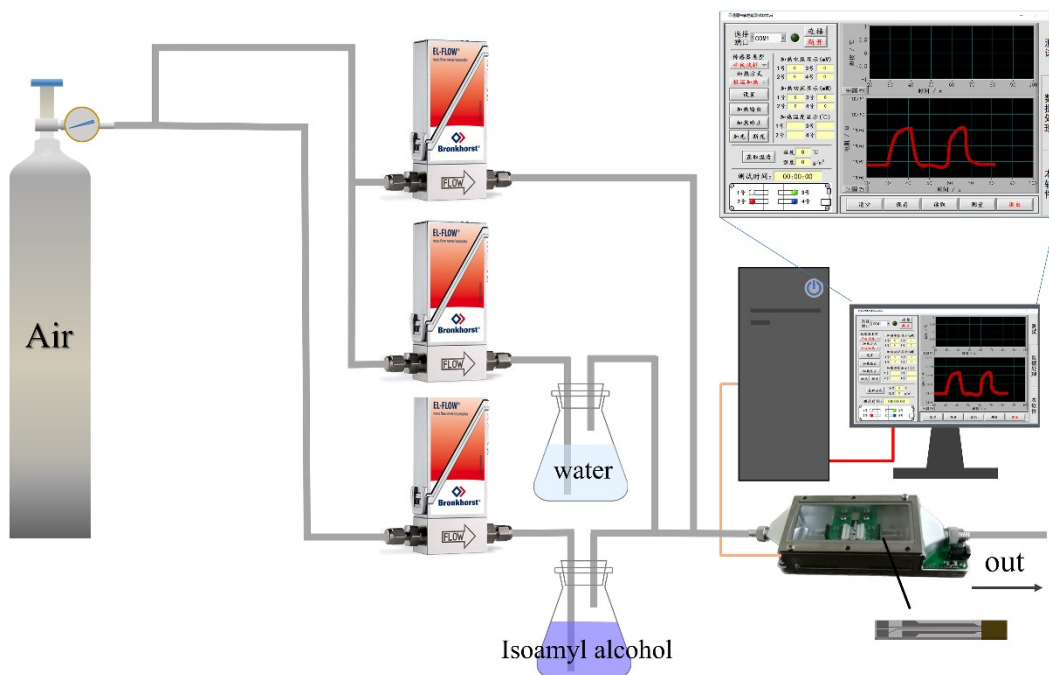


Figure S2. The schematic set-up of isoamyl alcohol sensing device.

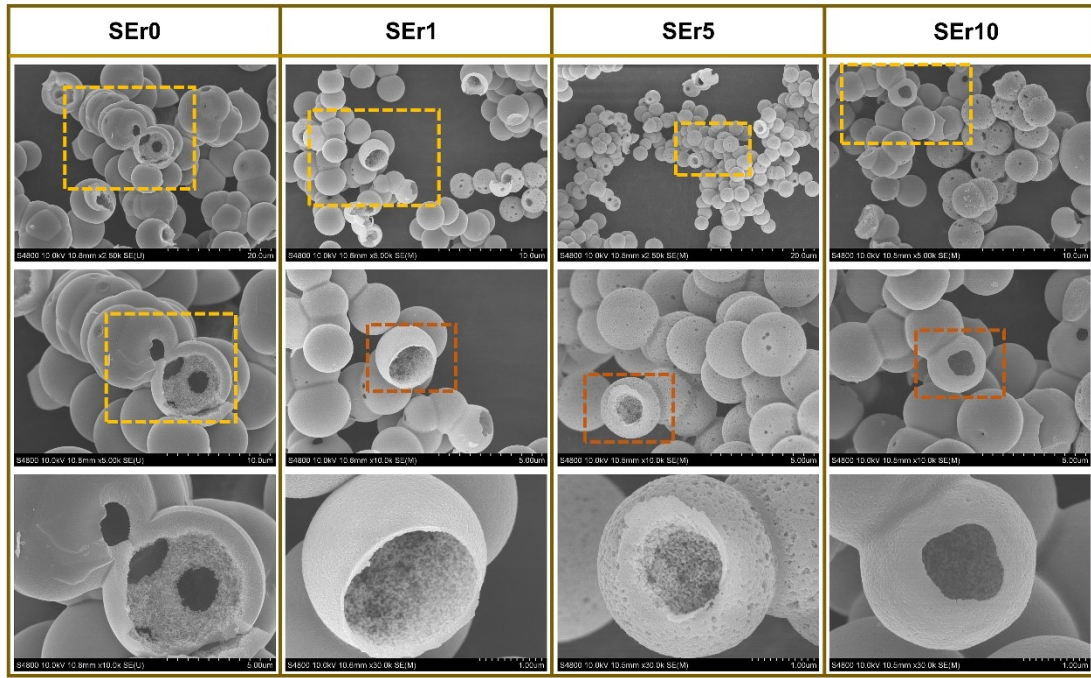


Figure S3. The FESEM images of as-prepared SEr0, SEr1, SEr5, SEr10 powders.

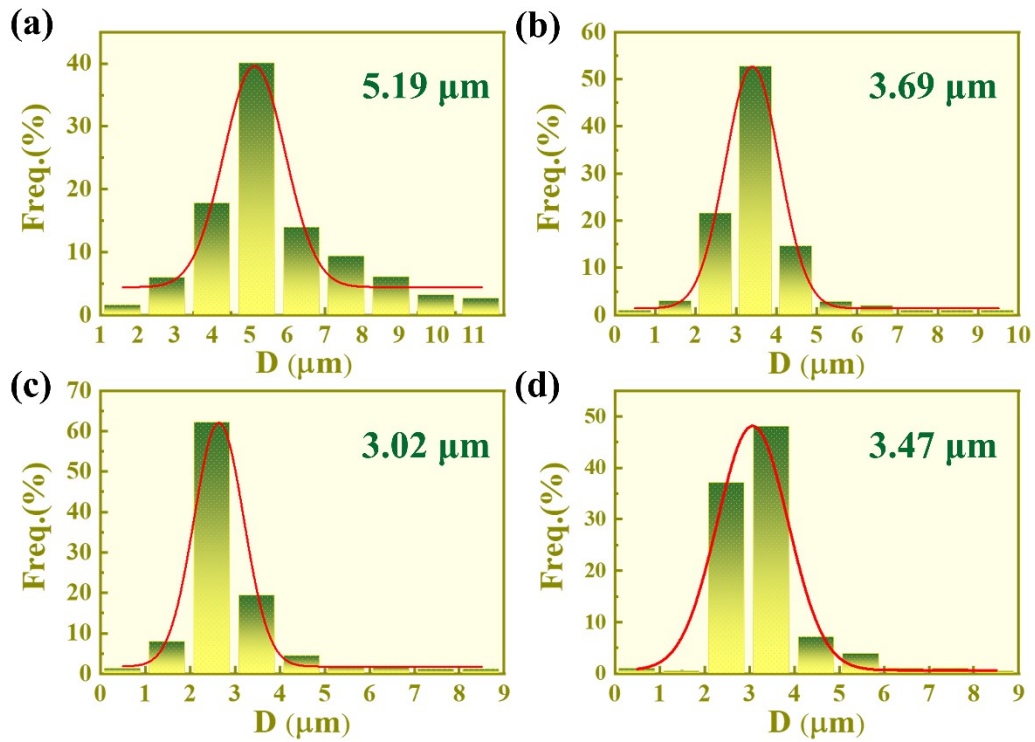


Figure S4. The particle size distribution of (a) SEr0, (b) SEr1, (c) SEr5, (d) SEr10.

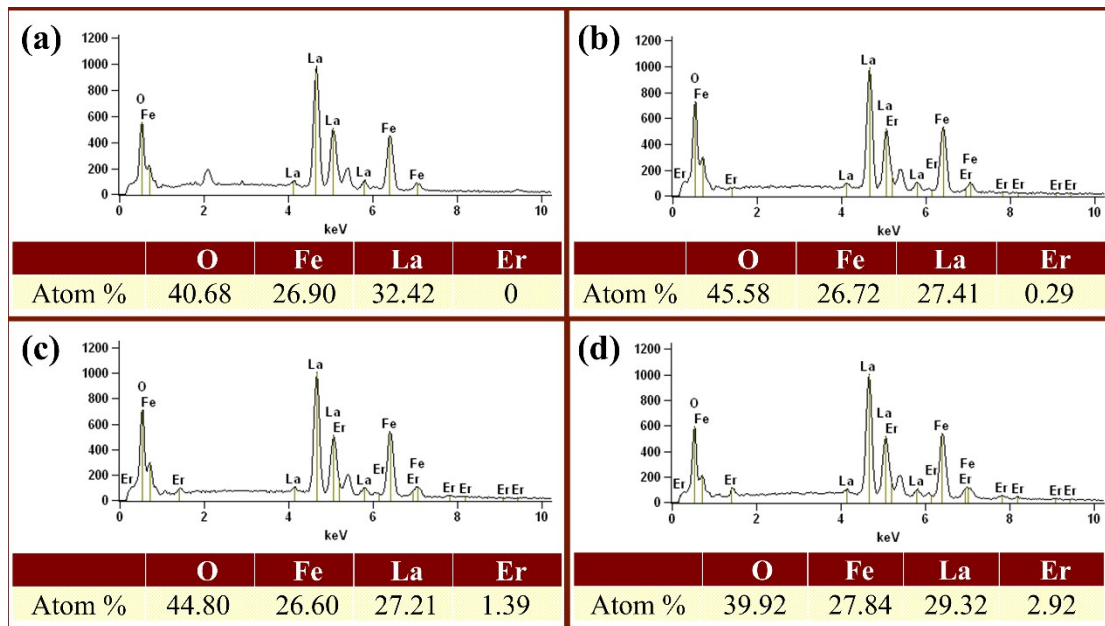


Figure S5. The EDS results of (a) SEr0, (b) SEr1, (c) SEr5, (d) SEr10.

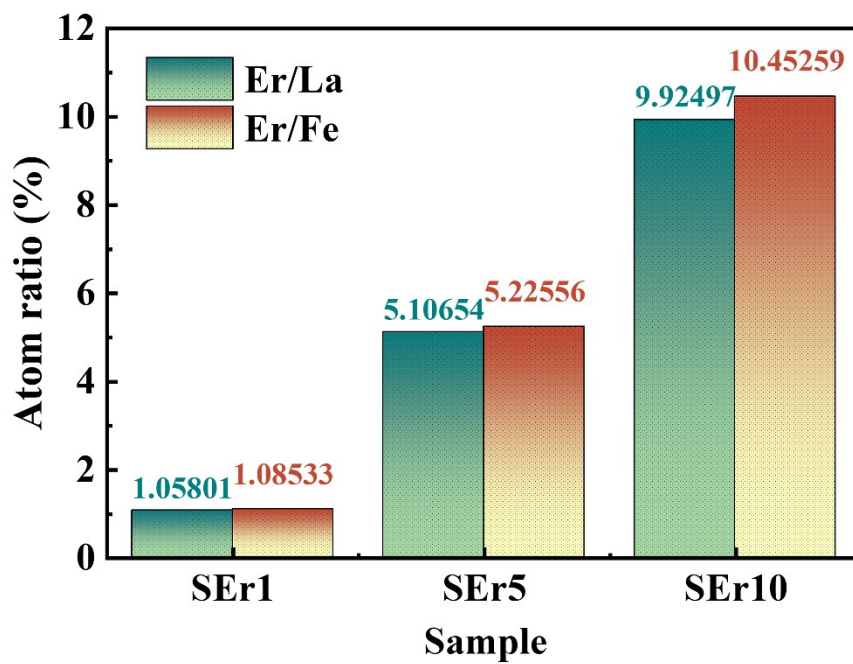


Figure S6. The Er: La and Er: Fe atom ratio of SEr1, SEr5, SEr10.

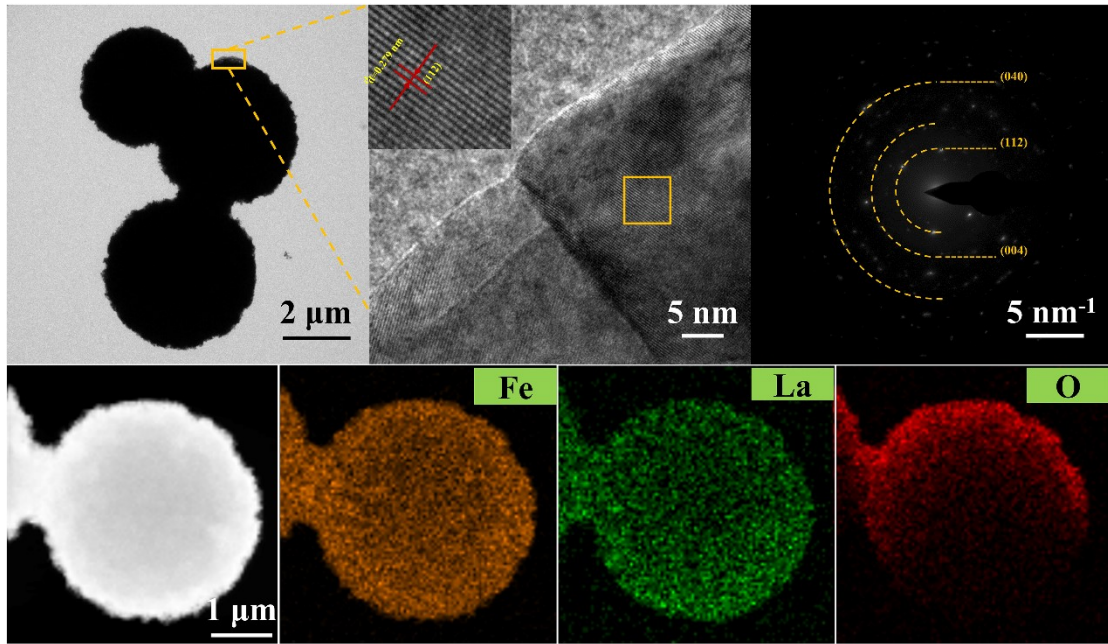


Figure S7. (a) TEM, (b) HRTEM, (c) SAED image and (d-g) EDX elemental mapping of SErO.

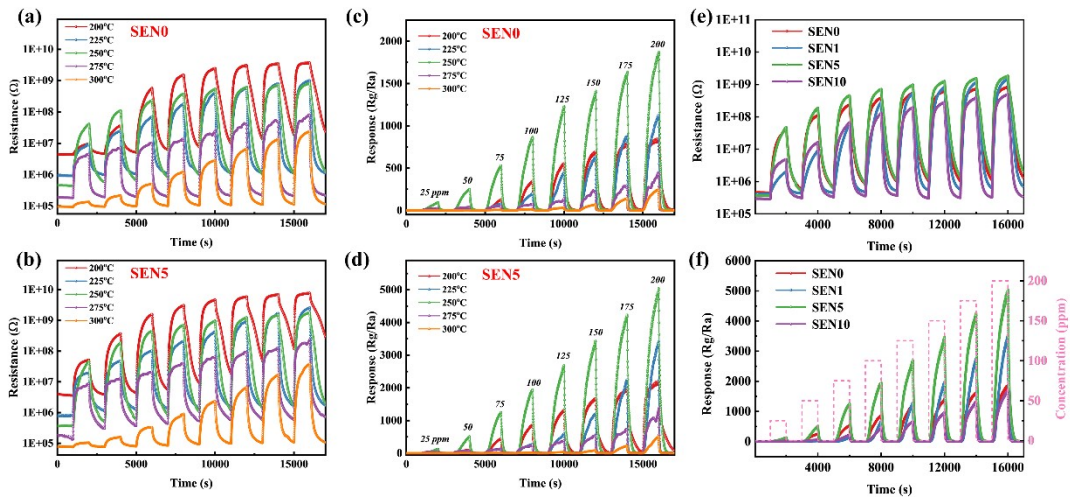


Figure S8. Dynamic resistance (a, b) and response (c, d) curves of SEN0 and SEN5 to various concentration of isoamyl alcohol at different temperature; (e) resistance change and (f) dynamic response curves of SEN0, SEN1, SEN5 and SEN10 to 25-200 ppm isoamyl alcohol at optimal operating temperature.

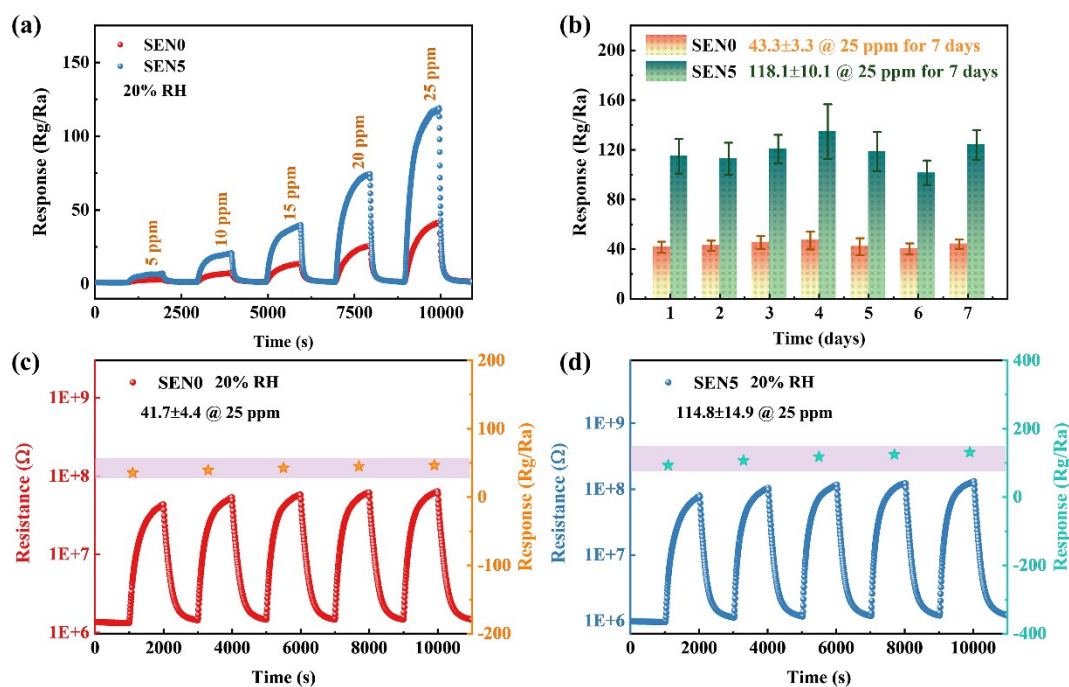


Figure S9. (a) Dynamic response curves of SEN0 and SEN5 to 5-25 ppm isoamyl alcohol; (b) the long-term stability of SEN0 and SEN5 at 25% RH; 5-cycles response curves of (c) SEN0 and SEN5 to 25 ppm.

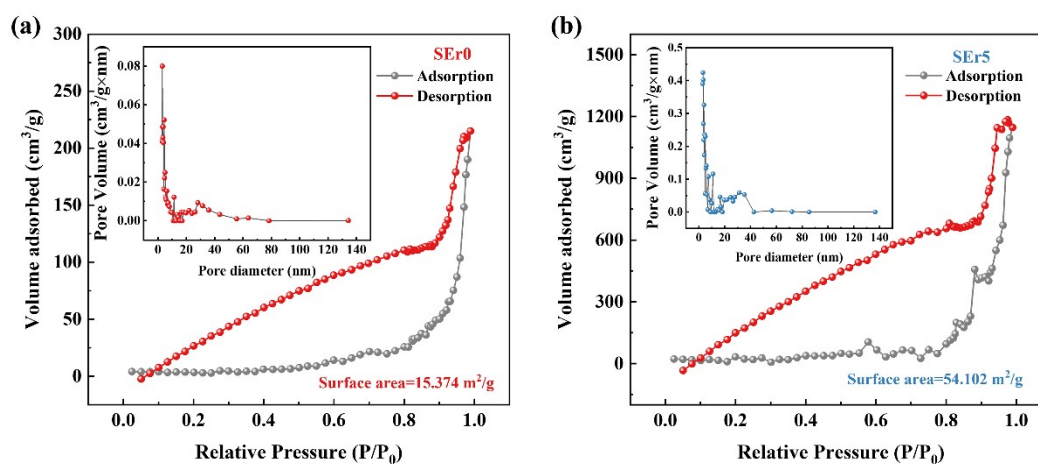


Figure S10. N_2 adsorption-desorption isotherms (inlet: pore-size distribution curve) of (a) SEr0 and (b) SEr5.

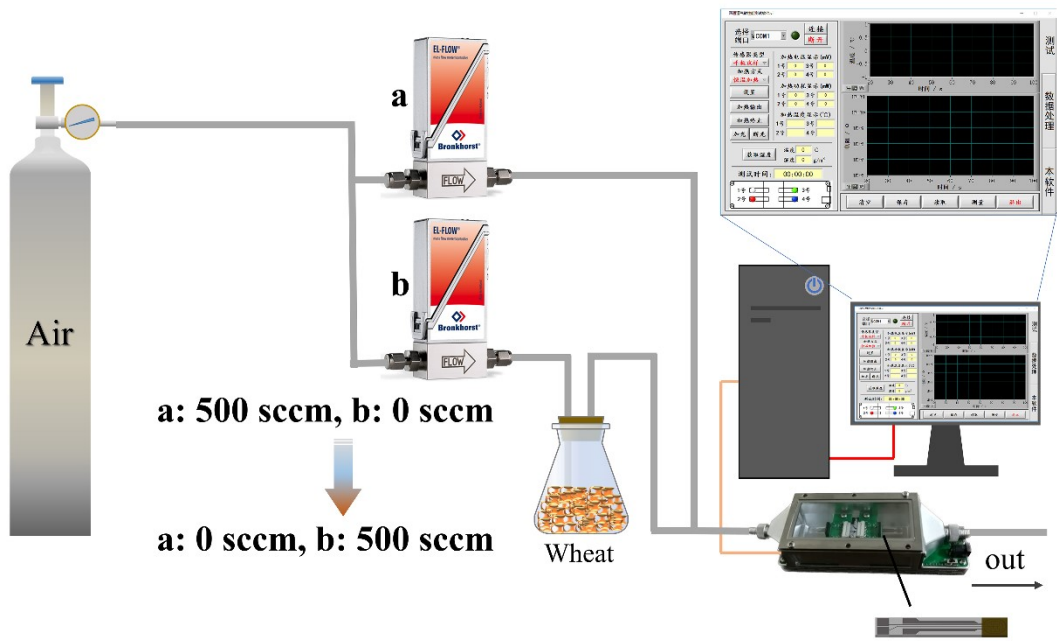


Figure S11. The schematic set-up of volatile gases detection from stored wheat.

Table S1. Physical properties of 0%, 1%, 5%, 10% Er doped LaFeO₃ calculated via XRD results.

Sample	SEr0	SEr1	SEr5	SEr10	Standard card 2θ (°)	Crystal index	Lattice spacing
	22.575	22.619	22.621	22.663	22.606	(002)	3.9301
	32.197	32.207	32.253	32.281	32.170	(112)	2.7802
Peak	39.579	39.715	39.761	39.768	39.702	(022)	2.2683
position	46.058	46.183	46.228	46.270	46.157	(004)	1.9650
2θ (°)	57.303	57.400	57.490	57.531	57.411	(204)	1.6037
	67.345	67.350	67.486	67.526	67.300	(040)	1.3901
	76.421	76.577	76.667	76.797	76.532	(116)	1.2438

Table S2. The position of the main peak and grain size of samples.

Sample	Peak position (°)	Grain size (nm)
SEr0	32.197	28.05
SEr1	32.207	23.25
SEr5	32.253	16.85
SEr10	32.281	20.68

Table S3. The results of ICP-AES.

Sample	Er (mg/L)	Er ($\times 10^{-3}$ mmol/L)	La (mg/L)	La ($\times 10^{-3}$ mmol/L)	Weight ratio (wt. %)	Atom ratio (at. %)
SEr1	0.603	3.61	40.36	290.55	1.49	1.24
SEr5	0.902	5.39	16.42	118.21	5.49	4.56
SEr10	4.983	29.79	41.94	301.92	11.88	9.87

Table S4. The fitting peak positions of La 3d region (XPS).

Peak position (eV)	La					
		3d _{3/2}			3d _{5/2}	
SEr0	855.05	852.60	850.69	838.26	835.76	833.93
SEr5	854.91	852.10	850.39	838.11	835.15	833.55

Table S5. The fitting peak positions of Fe 2p region (XPS).

Peak position (eV)	Fe				
	2p _{1/2} satellite	2p _{1/2}	2p _{3/2} satellite	2p _{3/2}	
SEr0	726.83	723.84	718.64	711.51	710.00
SEr5	725.96	723.65	718.56	711.55	710.00

Table S6. The fitting peak positions of O 1s and Er 4d region (XPS)

Peak position (eV)	O			Er	
	O _C	O _V	O _L	4d _{5/2}	
SEr0	531.50	531.05	529.14		
SEr5	531.35	530.89	529.17	169.50	167.43

Table S7. The isoamyl alcohol sensing properties of sensors.

Material	Method of preparation	Concentration (ppm)	Operation temperature (°C)	Response	Reference
NiO	Microwave-assisted solvothermal	100	250	2.8 (Ra/Rg)	5
Ru-QDs@g-CN	Thermal polymerization	100	30	55.2 (Rg/Ra)	6
CdS/MoS ₂	Hydrothermal	50	230	<50 (Ra/Rg)	7
CdS	Hydrothermal	50	190	50~75 (Rg/Ra)	8
Er doped LaFeO ₃	Hydrothermal	25	250	219.1 (Rg/Ra)	This work

Table S8. The band structure of SEr0 and SEr5.

Sample	E _g (eV)	E _{VB, NHE} (eV)	E _{CB, NHE} (eV)	Φ
SEr0	1.99	1.964	-0.026	6.921
SEr5	1.86	1.711	-0.149	7.047

References

1. G. Kresse and J. Furthmüller, *Comp. Mater. Sci.*, 1996, **6**, 15-50.
2. P. E. Blöchl, *Phys. Rev. B*, 1994, **50**, 17953-17979.
3. J. P. Perdew, J. A. Chevary, S. H. Vosko, K. A. Jackson, M. R. Pederson, D. J. Singh and C. Fiolhais, *Phys. Rev. B*, 1992, **46**, 6671-6687.
4. G. Stefan, A. Jens, E. Stephan and K. Helge, *J. Chem. Phys.*, 2010, **132**, 154104.
5. G. C. N. Vioto, T. M. Perfecto, C. A. Zito and D. P. Volanti, *Mater. Lett.*, 2023, **333**, 133641.
6. S. Samanta, P. Srinivasan, J. B. B. Rayappan and K. Kailasam, *Sens. Actuators, B*, 2022, **368**, 132060.
7. L. Liu, W. Yng, H. Zhang, X. Yan and Y. Liu, *Nanoscale Res. Let.*, 2022, **17**, 7.
8. X. Yan, W. Yang, C. Li, L. Liu and Y. Liu, *ACS Omega*, 2022, **7**, 1468-1476.